

## MULTI-PHASE FLUID CIRCULATION AND GROUND DEFORMATION: A NEW PERSPECTIVE ON BRADYSEISMIC ACTIVITY AT THE PHLEGREAN FIELDS (ITALY)

Micol Todesco,<sup>1</sup> Jonny Rutqvist,<sup>2</sup> Karsten Pruess,<sup>2</sup> and Curt Oldenburg<sup>2</sup>

1 INGV, Dip. Scienze della Terra e Geo-Ambientali, Università di Bologna  
P.zza P.ta San Donato,1, Bologna, I-40126, Italy

[todesco@geomin.unibo.it](mailto:todesco@geomin.unibo.it)

2 Earth Sciences Division, Lawrence Berkeley National Laboratory, Berkeley, CA 94720

### ABSTRACT

Like many caldera structures around the world, Phlegrean Fields caldera (Italy) periodically undergoes volcanic unrest, characterized by seismic activity and vertical ground displacement (bradyseism). These bradyseismic crises are usually interpreted as the product of pressure increment at the magma chamber level, but the existence of an important hydrothermal system in the area suggests that the migration of hot hydrothermal fluids should also play a role in the process. A complete description of the processes requires therefore a coupled analysis, accounting for both the flow of hot, multi-phase fluids and for the deformation of the porous medium. Here we applied the coupled thermo-hydro-mechanical model (TOUGH-FLAC) to study the role of hydrothermal circulation in ground deformation episodes at the Phlegrean Fields. Based on previous modeling results, we calculated the effects of an increased magmatic degassing on the deformation of a shallow elastic porous medium. Our results show that a short period of increased injection of deep fluid into the shallow hydrothermal system can represent a potential trigger for bradyseismic events, even in absence of a new magmatic recharge. Results also provided interesting insights on the complex interaction between fluid migration and ground deformation when phase changes are allowed. The comparison between these preliminary results and field data shows that the model captures both the temporal evolution of ground displacement and the compositional variations of fumarolic gas recently observed at the Phlegrean Fields.

### RECENT EVOLUTION AND MODELING EFFORTS AT PHLEGREAN FIELDS

The Phlegrean Fields is a large and widely urbanized volcanic district in southern Italy (Fig. 1). In historical times, this caldera structure has undergone remarkable episodes of ground deformation, accompanied by seismic activity. Secular subsidence is periodically interrupted by short-lasting uplift phases (Parascandola, 1947; Dvorak e Berrino, 1991; Dvorak e Gasparini, 1991; Dvorak e Mastrolorenzo, 1991). A renewal of eruptive activity may follow the maximum

uplift, as in the year 1538, when 7 m of vertical displacement preceded the Monte Nuovo eruption, the last recorded in the caldera (Dvorak e Gasparini, 1991).

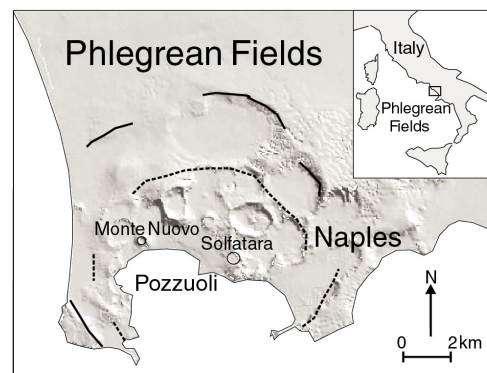


Fig. 1. The Phlegrean Fields caldera and its major collapsing structures: Campanian Ignimbrite (solid lines) and Neapolitan Yellow Tuff (dashed lines).

Other times, however, unrest crises do not culminate with eruptive activity, and terminate with a slow aseismic subsidence, as recently happened, in 1969-72 and 1982-84. Both episodes were confined within the central portion of the caldera, and were characterized by ca. 2 m of vertical displacement at the caldera centre (Caputo, 1979; Barberi et al., 1984; Berrino et al., 1984; Corrado et al., 1984). Since 1985, three minor uplift episodes interrupted a general trend of slow subsidence (Fig. 2). The region is also affected by intense hydrothermal activity, with surface manifestations concentrated within the ancient crater of Solfatara. Recent measurements of diffuse carbon dioxide emission through the soil revealed the impressive magnitude of this phenomenon. The energy budget associated with fluid ascent and shallow condensation was shown to be higher than the energy involved in recent seismic activity and ground deformation (Chiodini et al., 2001). Fumaroles, with a maximum discharge temperature of 164°C, are also present at La Solfatara and have been sampled during the last 20 years. Fluid composition (H<sub>2</sub>O, with CO<sub>2</sub>, H<sub>2</sub>S, N<sub>2</sub>, H<sub>2</sub>, and CH<sub>4</sub> as minor components) is typical

of the hydrothermal environment. The important contribution of magmatic components is apparent from the isotopic composition of H<sub>2</sub>O, CO<sub>2</sub>, and He (Tedesco et al., 1990; Allard et al., 1991; Panichi and Volpi, 1999; Tedesco and Scarsi, 1999).

Fumarolic gases underwent remarkable chemical changes during and after recent bradyseismic events (Barberi et al., 1984; Cioni et al., 1984; Martini, 1986; Martini et al., 1991; Tedesco and Scarsi, 1999). These variations were traditionally interpreted in terms of variable degree of boiling that would affect the hydrothermal system when heated by a new magma supply reaching the magma chamber.

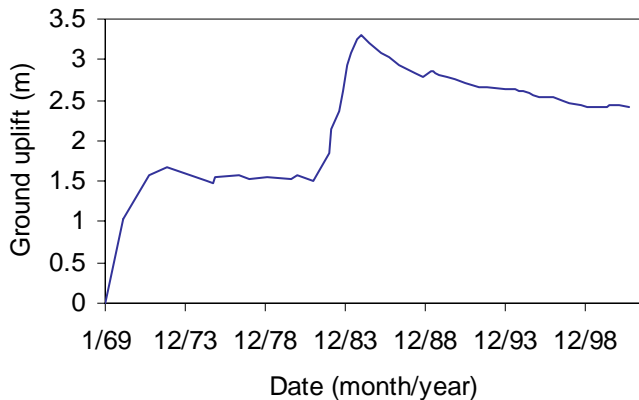


Fig. 2. Vertical ground displacement measured in Pozzuoli (Benchmark 25) since 1969.

The recent unrest phenomena have prompted new research efforts to unravel the mechanism driving bradyseismic crises. Several models have been proposed to explain the observed ground deformation, commonly in terms of pressure build-up inside a magma chamber (Caputo, 1976; Casertano et al., 1976; Corrado et al., 1976; Berrino et al., 1984; Bonafede et al., 1986; Bianchi et al., 1987). Most of these models describe the effect of a pressure source embedded in a homogeneous half space, with elastic or viscoelastic properties. Further models introduced the effects of structural discontinuities in controlling both the magnitude and the areal extent of ground deformation (De Natale and Pingue, 1993; De Natale et al., 1997; Orsi et al., 1999). The importance of fluids in bradyseismic crises was first recognized by Olivieri del Castillo and Quagliariello (1969), and later on by Casertano et al. (1976). More recently, other authors have recognized that purely mechanical models cannot fully explain the observed ground deformation and began to address the effects that heating and expansion of hydrothermal fluids can produce during a bradyseismic event (Bonafede, 1991; De Natale et al., 1991; 2001; Gaeta et al., 1998; Castagnolo et al., 2001). These models provided important insights but they are based on simplified descriptions of the fluid

dynamics, usually accounting for a steady, single phase fluid of constant properties.

On the other hand, a more realistic modeling of two-phase, two component hydrothermal fluid circulation at La Solfatara was performed recently (Tedesco et al. in press; Chiodini et al., *subm.*), with the TOUGH2 geothermal simulator (Pruess, 1991). These works could capture most of the main features characterizing the hydrothermal system at La Solfatara (Tedesco et al., in press) and its recent compositional variations (Chiodini et al., *subm.*). However, they did not account for the deformation of the solid porous matrix.

The present work represents a natural evolution of the previous modeling, and it is aimed at coupling the fluid-dynamics of hydrothermal circulation to a mechanical analysis of the porous media. The simulations presented here are based on the results described in Tedesco et al. (in press), that we shall briefly recall hereafter. The work was focused on the shallower portion of the hydrothermal system of La Solfatara, from the surface to a depth of 1500 m. This shallow system was heated by a continued inflow of a hot mixture of water and carbon dioxide, representing the product of deep magmatic degassing. Upon prolonged injection, a large plume of hot fluids develops and a single-phase gas region forms at shallow depths, as predicted by the independent geochemical model (Chiodini and Martini, 1998). The composition and physical condition of this single-phase gas region correspond to those inferred from geochemical data for the source region feeding the fumarolic activity (Tedesco et al., in press).

The same model was then applied to simulate subsequent unrest crises at La Solfatara (Chiodini et al., *subm.*), by means of discrete periods during which the injection rate of the deep fluid at the source was increased. The model successfully reproduced the observed chemical variation, all preceded by an increase of pore pressure and temperature.

## **MODELING OF FLUID INJECTION AND GROUND DEFORMATION**

Further insights into the phenomena driving bradyseismic events may be achieved with a more complex approach, in which both the dynamics of multi-component hydrothermal circulation and the mechanical aspects are considered. The coupled TOUGH-FLAC model applied here links the capabilities of the TOUGH2 geothermal simulator (Pruess, 1991) with the geotechnical analysis of rock and soil performed with FLAC3D, a commercial code for rock mechanics (Itasca Consulting Group Inc., 1997). Both codes are fully described elsewhere, as is their coupling (Rutqvist et al., 2002). Briefly, TOUGH2 describes the coupled transport of heat and multi-phase, multi-component fluids through a porous matrix, accounting for phase changes and associated

latent heat effects. The fluid components considered here are water and carbon dioxide. FLAC3D is an explicit finite difference program applied here to describe the coupled thermomechanical behavior of a continuous elastic medium, as it reaches equilibrium. The coupled TOUGH-FLAC model was applied to study the mechanical effects potentially induced by an intensified magma degassing. Starting from the present system conditions, calculated following Todesco et al. (in press), bradyseismic crises are here simulated by temporarily increasing the injection rate at the fluid source. Composition and temperature of the injected fluid mixture were unchanged.

The coupled model allowed us to first calculate the effects of increased injection rate on overall fluid circulation and phase distribution, and then to estimate the corresponding rock deformation, arising from temperature and pore pressure changes. At this stage, we did not take advantage of the full (two-way) THM coupling allowed by the code. In other words, we did not calculate the effects that changes in stress distribution would have on rock porosity and permeability. This decision was based on methodological considerations, suggesting to address a simplified problem before dealing with more complex interactions, but was also due to the lack of necessary information on the relationship linking stress distribution, and rock porosity and permeability for the rock of the Phlegrean Fields.

To allow for the coupling with FLAC3D, all simulations were run in a three-dimensional domain, whose geometry and dimensions were chosen to match previous models. We here consider the inner portion of the Phlegrean Fields caldera, bounded by the Neapolitan Yellow Tuff collapsing structures (Fig.1). Thanks to the problem's symmetry, the computational domain represents 1/4th of the caldera (Fig. 3). As in Todesco et al. (subm), only the shallower portion of the hydrothermal system was considered. This was necessary to keep the simulation within the modeling assumptions and, as a consequence, thermal effects associated with the deeper portion of the system are neglected. At this stage, we therefore expect to reproduce only a fraction of the observed deformation. In all simulations we performed, the fluid is a mixture of water and carbon dioxide and rock physical properties are considered to be homogeneous and constant, and are reported in Table 1. Two values for the rock elastic properties were chosen based on literature data.

## NUMERICAL SIMULATION

Initial conditions were calculated with TOUGH2, as in Todesco et al. (in press), simulating a prolonged (4000 years) injection of water and carbon dioxide from a source area (150x150 m) at the base of the domain

(Fig. 4). The composition of the fluid mixture ( $\text{CO}_2/\text{H}_2\text{O}=0.2$  vol%) was taken to be representative of recent fumarolic emissions.

Table 1. Physical and elastic properties of the porous medium.

Rock Physical Property	
Density ( $\text{kg/m}^3$ )	2000
Thermal Conductivity ( $\text{W/m}^\circ\text{C}$ )	2.8
Specific heat ( $\text{J/kg}^\circ\text{C}$ )	1000
Bulk modulus K (GPa)	5 - 10
Shear modulus G (GPa)	2 - 5

The injection rates (1500 tons/day of  $\text{CO}_2$  and 3000 tons/day of  $\text{H}_2\text{O}$ ) were arbitrarily chosen to be consistent with the diffuse degassing rate measured at the surface (Chiodini et al., 2001).

No heat and fluid flow is allowed through the bottom and lateral boundary, whereas the upper boundary is open and at fixed atmospheric pressure and temperature.

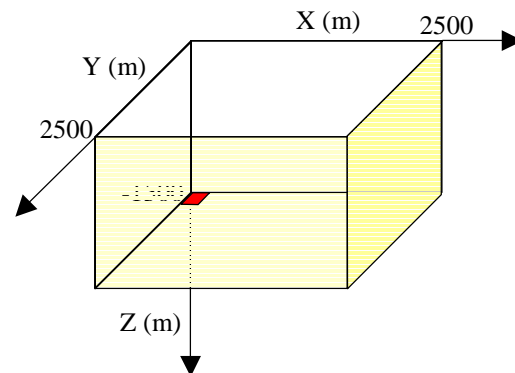


Fig. 3. Computational domain for the coupled TOUGH-FLAC simulation. Source region (150x150m) is indicated in red.

The system conditions thereby achieved were also used to calculate the corresponding mechanical equilibrium that was, in turn, applied as initial conditions for the mechanical problem. In the FLAC simulations, roller boundaries (zero horizontal displacement) are assigned along the lateral boundaries, representing the fault system associated with the Neapolitan Yellow Tuff eruption. Zero (vertical) displacement is also assigned along the bottom boundary.

## TOUGH2 results

Two TOUGH2 simulations were run in which the injection rate of deep fluid was increased for a period of 2 years. Simulations were then continued to a final time of 35 years. In the first case (Simulation 5x) the

injection rate is increased 5 times, whereas in the second case (Simulation 10x) the injection rate during the first 2 years is increased by a factor 10. The composition of the injected fluids does not change over the simulation time, nor does their temperature.

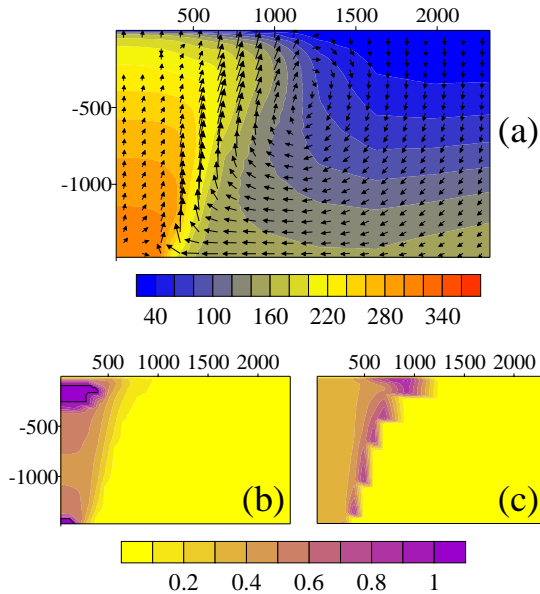


Fig. 4. Initial conditions on the XZ plane. (a) Temperature ( $^{\circ}\text{C}$ ) and liquid flow; (b) gas saturation (solid line: gas fraction = 1); (c) gas composition ( $\text{CO}_2$  mass fraction).

In both simulations, the increased injection rate generates similar effects on fluid circulation. The following figures refer to the Simulation 10x, where changes are more evident, but similar observations can be made for Simulation 5x. As a consequence of higher fluid injection rate, fluid pressure near the source increases (Fig. 5). Over time the region affected by overpressure becomes larger and reaches shallower depths. Pressure difference increases to a maximum value (12 MPa, in 1 year in Simulation 5x; 20 MPa after 6 months in Simulation 10x), and then gradually dissipates with time. After the period of enhanced injection rate, an overpressure of 0.5 MPa is still felt in both simulations at shallow depth (<400 m).

Thanks to the higher injection rate, the two-phase plume becomes larger, mainly at its base. The clockwise convective cell, initially characterizing the liquid flow, is destroyed as fluid acquires a radial motion, from the source outward, that is maintained for the first 2 years of simulation (Fig. 6). The temperature also undergoes a remarkable increase, despite the fact that injection temperature is unchanged.

Part of this increment is associated with the plume enlargement, as hot fluids reach greater distances from the source and heat up an initially colder region.

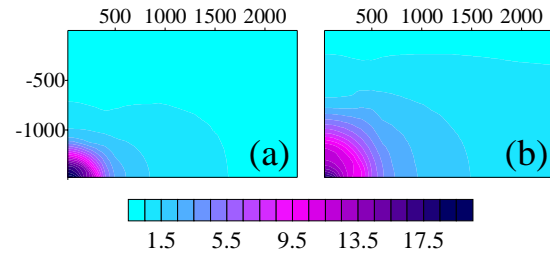


Fig. 5. Simulation 10x. Pressure difference (MPa) with respect to the initial value, after 6 months (a) and 24 months (b) of simulation

Heating, however, occurs also near the source: overpressure here leads to vapor condensation, and hence to the release of latent heat. The temperature increment is accompanied by a reduction of the volumetric gas fraction in the region and by an increase of carbon dioxide mass fraction in the gas phase (Fig. 6). A front of carbon-dioxide-rich gas forms above the source, and progressively moves upward.

After 2 years, fluid injection rate is reduced to its initial value, and the simulation is continued to a final time of 35 years.

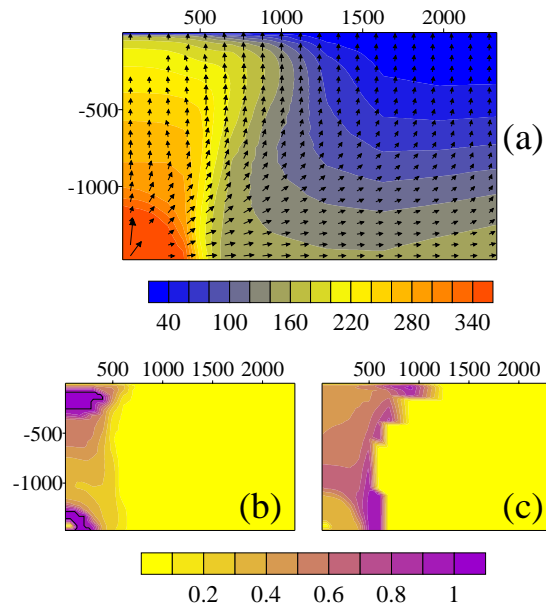


Fig. 6. Simulation 10x. (a) Temperature ( $^{\circ}\text{C}$ ) and liquid flow; (b) gas saturation (solid line: gas fraction = 1); (c) gas composition ( $\text{CO}_2$  mass fraction), after 1 year of simulation.

Fluid pressure quickly drops above the source, and within 10 years a slight decompression with respect to initial value is observed. Despite this general decline, a minor pressure front (+ 4 MPa, with respect to the initial conditions) still persists and propagates upwards (Fig. 7).

One year after the injection rate has been reduced, the outward motion of main fluid flow is still preserved. It

takes 5 years (3 years of reduced injection) to observe a change in the fluid flow pattern (Figure 8a). At this time, the liquid flows from the outer region of the domain toward the fluid source, where pressure is relieved, while it is driven away from the region where overpressure still exists, generating a rather complex flow pattern.

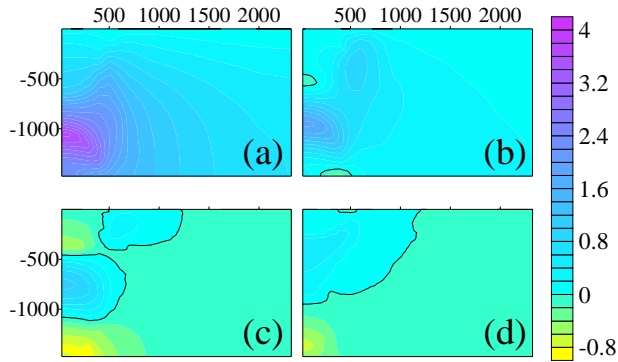


Fig. 7. Simulation 10x. Pressure difference (MPa) with respect to the initial value after (a) 3 years, (b) 5 years, (c) 10 years, and (d) 35 years. Solid line: pressure difference=0.

At the end of the simulation, the main clockwise convective cell characterizing the initial condition is established again.

As fluid injection rate is reduced, water boiling occurs as a consequence of lower fluid pressure. The single phase gas region at the source level enlarges significantly upwards (Fig. 8b). The boiling front is nicely highlighted by the distribution of the mass fraction of carbon dioxide in the gas phase (Fig. 8c). At the same time, the fluids injected during the first 2 years are rising, and causing the plume enlargement at progressively shallower depth. Gas fraction therefore increases also along the edge of the plume. The regions where gas fraction increases above its initial value undergo a slight increase in fluid pressure.

Temperature is somewhat reduced by the boiling process, but a thermal front still exists above the source, where temperature is some tens of degrees higher than initially.

After 10 years of simulation, shrinking of the plume becomes evident near the fluid source in both simulations, while at shallower depths the effects of the high injection rate period are still evident. The shallow single phase gas region is pushed upward by the rising fluids and its size is slightly reduced, as the plume progressively shrinks.

The distribution of temperature, gas fraction and composition at the end of the simulation are depicted in Figure 9. The plume's shape and phase distribution are significantly different than initially. Gas fraction is higher near the base of the plume, where the single

phase gas zone reaches shallower depths within the plume.

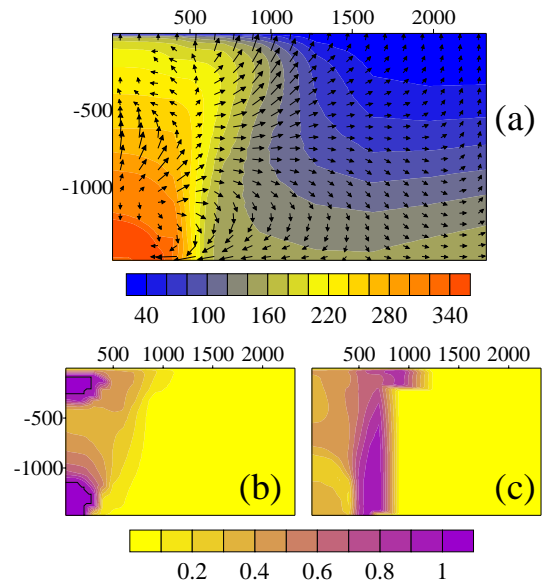


Fig. 8. Simulation 10x. (a) Temperature ( $^{\circ}\text{C}$ ) and liquid flow pattern. (b) volumetric gas fraction, and (c) gas composition, after 5 years of simulation

Gas composition within the central portion of the plume is similar to the initial value, with carbon dioxide reaching maximum mass fraction along the outer edge of the larger plume. The shallow single-phase gas region is greatly reduced and slightly shifted toward shallower depth.

As a consequence of these changes in phase distribution and composition, also the single phase gas region undergoes changes of gas composition. Accordingly, fumarole emissions that are fed by this single-phase gas reservoir are also expected to change their composition.

### FLAC3D results

In this section we shall examine how the described evolution of the fluid circulation affects the porous matrix, in terms of vertical displacement.

The pressure and temperature fields calculated with TOUGH2 at different times were fed to FLAC3D to calculate the associated stress and strain fields. Changes induced by the increased fluid injection rate are here shown in terms of vertical displacement. The rock deformations induced in the two cases of Simulation 5x and 10x are similar, being characterized by the same evolution, with significantly stronger displacements for the 10x case (Figures 10 and 11).

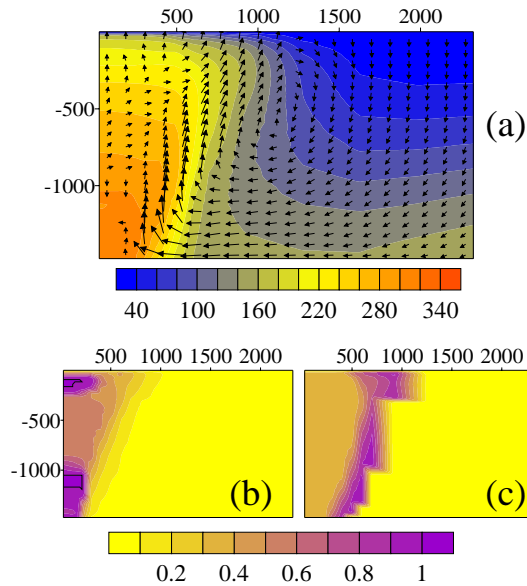


Fig. 9. Simulation 10x. (a) Temperature ( $^{\circ}\text{C}$ ) and liquid flow, (b) volumetric gas fraction, and (c) gas composition, after 35 years of simulation

As pressure and temperature increase above the fluid source, rock deformation occurs, mainly driven by the temperature increment. The maximum vertical displacement is reached at the top of the heated region, and becomes progressively shallower as the thermal front rises.

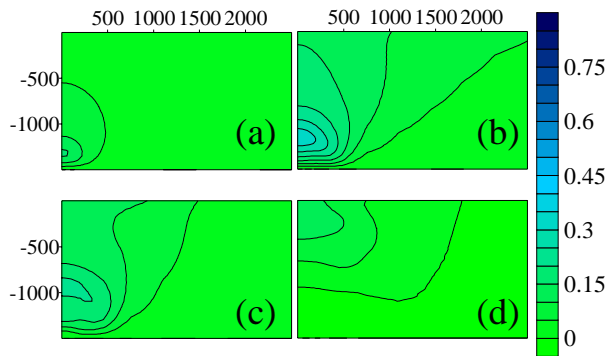


Fig. 10. Simulation 5x. Vertical displacement (m), after: (a) 6 months; (b) 2 years; (c) 5 years; (d) 35 years of simulation. Contours every 0.05 m.

Deformation increases progressively during the high injection rate period, at the end of which the maximum vertical displacement is reached. The region affected by rock deformation becomes larger with time, as the pressure and temperature fronts propagate, and after 6 months of simulation, some vertical displacement affects the surface.

In Simulation 5x, the maximum vertical displacement is 0.34 m and is reached at a depth of 1150 m. When

the injection rate is reduced, rock deformation is quickly relieved. As mentioned above, pressure and temperature decrease sharply, but minor fronts of overpressure and thermal anomaly survive, and slowly migrate upward. Similarly, the maximum vertical displacement is reduced (0.21 m and 0.12 m, after 5 and 35 years of simulation respectively), while its position continues to rise toward the surface.

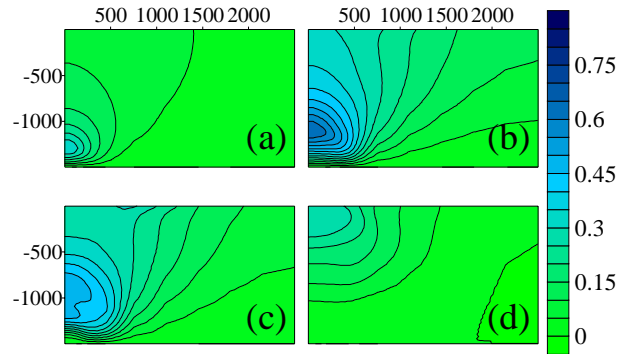


Fig. 11. Simulation 10x. Vertical displacement (m), after: (a) 6 months; (b) 2 years; (c) 5 years; (d) 35 years of simulation. Contours every 0.05 m.

Displacements calculated for Simulation 10x show a similar evolution, but higher absolute values (Figure 11). Again the maximum value (0.64 m) is attained at the end of the high injection rate period. Then deformation drops to 0.48 m (after 5 years) and to 0.28 m at the end of the simulation.

As the deformation slowly propagates upward, two different effects are recognizable, especially in the Simulation 10x. As mentioned above, during the high injection period a thermal front develops that is responsible for rock deformation. When fluid injection is reduced, boiling occurs above the fluid source. As a consequence, the temperature there is somewhat reduced. The former thermal anomaly is thereby split in two by this colder layer. The corresponding deformation is therefore also characterized by two maxima (Fig. 12): one corresponding to the upper thermal front, where also the maximum pressure gradient is observed, and a second one associated with the inner portion of the heated region. With time, the two points of maximum deformation rise and merge together, as they reach the surface, in about 20 years. At this time, the vertical displacement is significantly reduced but it can still produce a second phase of uplift, that still goes on at the end of the simulation (35 years).

The second effect is associated with shallow heating. This phenomenon begins before the injection rate is reduced and is initially due to the propagation of the pressure front. After 2 and 3 years of simulation, the overpressure generates some degree of condensation

near the surface, along the outer edge of the plume (ca. 700 m from the symmetry plane).

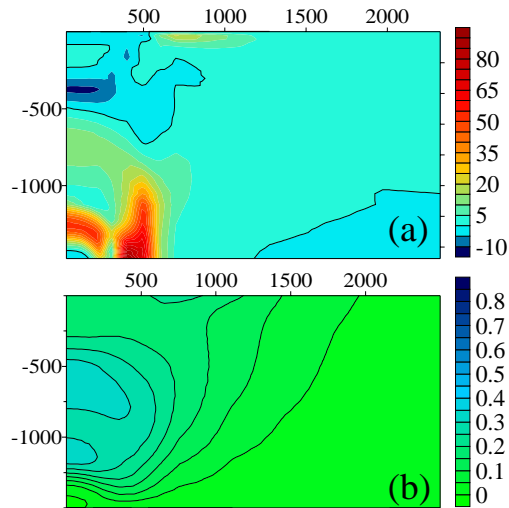


Fig. 12. Simulation 10x. (a) Temperature difference ( $^{\circ}\text{C}$ ) with respect to initial distribution. Solid line: temp. difference =0; (b) Vertical displacement (m), contours every 0.05 m. After 10 years of simulation

As a consequence, temperature at this location undergoes a slight increase, still persistent after 10 years (Fig.12a). Such heating generates some vertical displacement near the surface, at some distance from the symmetry axis.

Because of this evolution, vertical displacement at the surface displays a rather complex behaviour (Fig. 13). For Simulation 10x, uplift initially involves the central part of the domain, and progressively increases during the first 2 years of high injection rate, to a maximum value (at the surface) of 0.32 m. Then subsidence takes place, when the injection rate is reduced and the plume is not sustained anymore. At the same time, uplift begins along the outer edge of the plume, reaching a maximum value of 0.24 m, after 10 years. Also this deformation progressively declines, as the pressure front dissipates with time and the temperature goes back to initial values. Then, perturbations induced at depth, during the high injection rate period, rise along the domain, and reach the surface in about 20 years. A second phase of central uplift is then observed at the surface. This second uplift progressively increases and reaches a maximum value of 0.26 m at the end of the simulation.

A similar evolution is observed for Simulation 5x at the end of the high injection rate period, the maximum vertical displacement at the surface is 0.15 m. Also in this case, a “distal” uplift is observed at about 700 m from the symmetry plane. Maximum vertical

displacement (0.10 m) is reached after 10 years of simulation.

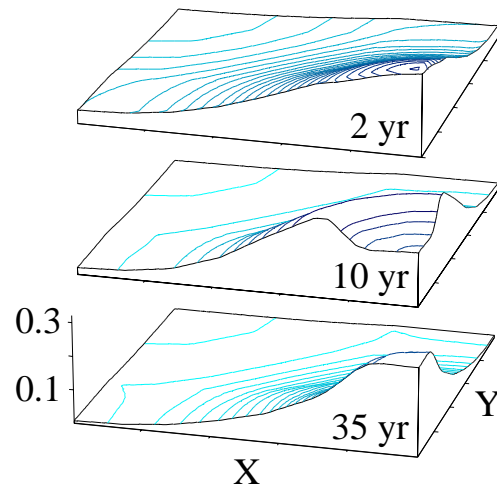


Fig. 13. Simulation 10x. Vertical displacement (m) at the surface, at different times. X and Y axis range from 0 to 2500 m.

Finally, the second uplift, corresponding to the ascent of the deep pressure and thermal front, reaches a value of 0.11 m, after 35 years.

Slightly higher values of ground displacement are obtained if lower values of the elastic constants are considered (Simulation 10x(s), Fig. 14). The evolution is quite similar to that described previously, but the maximum deformation at the end of the high injection rate period is increased to 0.83 m, again located at -1100 m. The corresponding surface displacement is 0.48 m. Uplift in lateral position is again observed, reaching a maximum value of 0.25 m after 10 years of simulation. After 35 years, the maximum vertical displacement at the surface is 0.28 m.

The described fluid flow evolution and the corresponding surface deformation can be compared with the available measured data from the field. Figure 15 shows the temporal evolution of vertical displacement at the caldera center (Pozzuoli, Benchmark 25), and the simultaneous variation in chemical composition recorded at La Solfatara fumarolic field. According to Chiodini et al. (subm), the recent evolution of these two parameters derives from a series of discrete episodes of enhanced magmatic degassing. As we are here simulating only one of these episodes, we focus on the most recent large bradyseismic event, and particularly on the period 1983-1998. Vertical displacement is normalized with respect to the maximum value over this period. Chemical composition is expressed in terms of  $\text{CO}_2/\text{H}_2\text{O}$  ratio, normalized with respect to its initial value (ca. 0.21 vol-%).

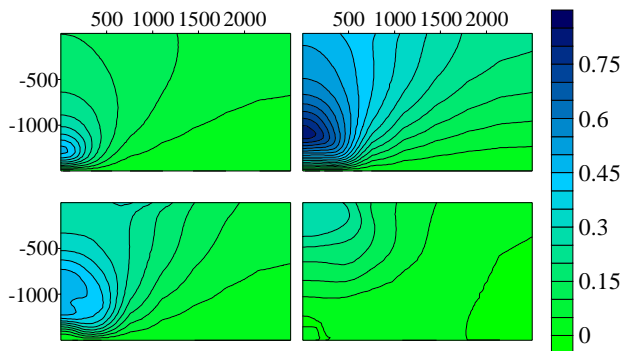


Fig. 14. Simulation 10x(2).  $K=5\text{Gpa}$ ;  $G=2\text{Gpa}$ . Vertical displacement (m) after (a) 6 months; (b) 2 years; (c) 5 years; (d) 35 years. Contours every 0.05 m.

As expected, absolute values of ground deformation are underestimated by our model, which accounts only for the shallower portion of the hydrothermal system. As Figure 15 shows, the model captures both the uplift phase and the subsequent slower subsidence that could not be explained by traditional models involving magma chamber overpressure.

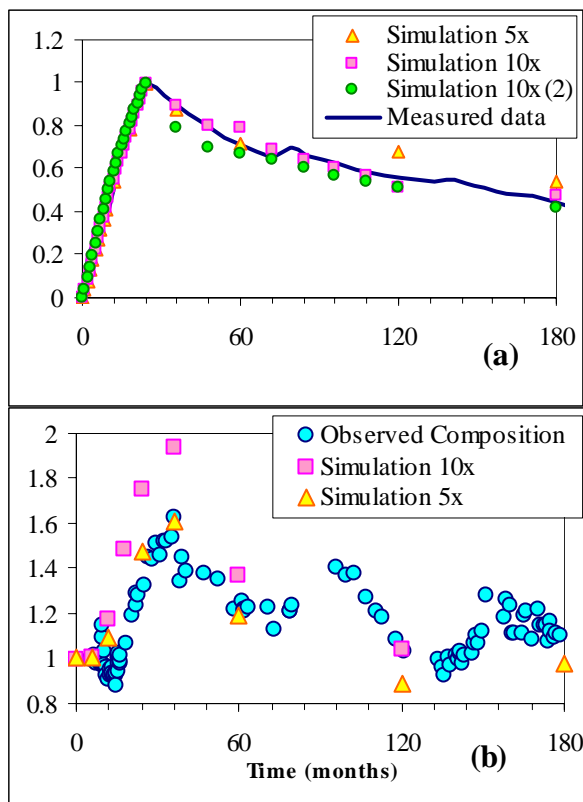


Figure 15. Comparison between data and simulation results: (a) normalized vertical displacement; (b) chemical composition.

The model also reproduces the observed chemical changes, despite the fact that no chemical variations were prescribed at the source. The match between calculated and observed composition is good for the first 5 years, after which a new period of high injection rate began (Chiodini et al., subm).

Further simulations are planned for the future, to account for different boundary conditions.

Preliminary results presented here confirm that periods of intense magmatic degassing can represent an effective triggering mechanism for recent bradyseismic events, explaining many observed features.

## ACKNOWLEDGEMENT

The first author was financed by the Gruppo Nazionale Vulcanologia, of the Istituto Nazionale di Geofisica e Vulcanologia (Italy). The LBNL authors were supported by the Assistant Secretary for Energy Efficiency and Renewable Energy, Office of Geothermal Technologies, of the U.S. Department of Energy under contract No. DE-AC03-76SF00098.

## REFERENCES

- Allard, P., Maiorani, A., Tedesco, D., Cortecchi, G. and Turi, B. (1991), "Isotopic study of the origin of sulfur and carbon in Solfatara fumaroles, Campi Flegrei caldera", *Journal of Volcanology and Geothermal Research*, **48**, 139-159.
- Barberi, F., Corrado, G., Innocenti, F. and Luongo, G. (1984), "Phlegrean Fields 1982-1984: brief chronicle of a volcano emergency in a densely populated area", *Bulletin of Volcanology*, **47**, 175-185.
- Bianchi, R., Corradini, A., Federico, C., Giberti, G., Lanciano, P., Pozzi, J.P., Sartoris, G. and Scandone, R. (1987), "Modelling of surface ground deformation in volcanic areas: the 1970-1972 and 1982-1984 crises of Campi Flegrei, Italy", *Journal of Geophysical Research*, **92** (B13), 14139-14150.
- Bonafede, M. (1991), "Hot fluid migration, an efficient source of ground deformation, application to the 1982-1985 crisis at Campi Flegrei-Italy", *Journal of Volcanology and Geothermal Research*, **48**, 187-198.
- Bonafede, M., Dragoni, M. and Quarenì, F. (1986), "Displacement and stress field produced by a centre of dilatation and by a pressure source in a viscoelastic half-space: application to the study of ground deformation and seismic activity at Campi Flegrei, Italy", *Geophysical Journal of the Royal Astronomic Society*, **87**, 455-485.
- Caputo, M. (1979), "Two thousands years of geodetic and geophysical observations in the Phlegrean Fields near Naples", *Geophysical Journal of the Royal Astronomic Society*, **56**, 319-328.
- Casertano, L., Olivieri del Castello, A. and Quagliariello, M.T. (1976) "Hydrodynamics and geodynamics in the Phlegrean Fields area of Italy", *Nature*, **264**, 161-154.
- Castagnolo, D., Gaeta, F.S., De Natale, G., Peluso, F., Mastrolorenzo, G., Troise, C., Pingue, F. and Mita D.G. (2001), "Campi Flegrei unrest episodes and possible evolution towards critical phenomena", *Journal of Volcanology and Geothermal Research*, **109**, 13-30.
- Chiodini, G. and Marini, L. (1998), "Hydrothermal gas equilibria: the  $\text{H}_2\text{O}-\text{H}_2-\text{CO}_2-\text{CO}-\text{CH}_4$  system", *Geochimica et Cosmochimica Acta*, **62** (15), 2673-2687.

- Chiodini, G., Frondini, F., Cardellini, C., Granieri, D., Marini, L. and Ventura, G. (2001), "CO<sub>2</sub> Degassing and Energy Release at Solfatara Volcano, Campi Flegrei, Italy", *Journal of Geophysical Research*, **106**, 16213-16221.
- Chiodini, G., Todesco, M., Caliro, S., Del Gaudio C., Macedonio, G. and Russo M. (subm), "Magma degassing as a trigger of bradyseismic events: the case of Phlegrean Fields (Italy)". Submitted to *Geophysical Research Letters*.
- Cioni, R., Corazza, E. and Marini, L. (1984), "The gas/steam ratio as indicator of heat transfer at the Solfatara fumaroles, Phlegrean Fields (Italy)", *Bulletin of Volcanology*, **47**, 295-302.
- Corrado, G., Guerra, I., Lo Bascio, A., Luongo, G. and Rampoldi, R. (1976), "Inflation and microearthquake activity of Phlegrean Fields, Italy", *Bulletin of Volcanology*, **40** (3), 169-188.
- Corrado, G., Luongo, G. and Toro, B. (1984), "Ground deformation and gravity change accompanying the 1982 Pozzuoli uplift", *Bulletin of Volcanology*, **47** (2), 187-200.
- De Natale, G. and Pingue, F. (1993), "Ground deformation in collapsed caldera structures", *Journal of Volcanology and Geothermal Research*, **57**, 19-38.
- De Natale, G., Petrazzuoli, S.M. and Pingue, F. (1997), "The effects of collapse structures on round deformation in calderas", *Geophysical Research Letters*, **24**(13), 1555-1558.
- De Natale, G., Pingue, F., Allard, P. and Zollo, A. (1991), "Geophysical and geochemical modeling of the 1982-1984 unrest phenomena at Campi Flegrei caldera (southern Italy)", *Journal of Volcanology and Geothermal Research*, **48**, 199-222.
- De Natale G., Troise C. and Pingue, F. (2001), A mechanical fluid-dynamical model for ground movements at Campi Flegrei caldera", *Journal of Geodynamics*, **32** (4-5), 487-517.
- Dvorak, J.J. and Gasparini, P. (1991), "History of earthquakes and vertical ground movements in Campi Flegrei caldera, Southern Italy: a comparison of precursor events to the A.D. eruption of Monte Nuovo and of activity since 1968", *Journal of Volcanology and Geothermal Research*, **48**, 77-72.
- Dvorak, J.J. and Mastrolorenzo, G. (1991), "The mechanism of recent vertical crustal movements in Campi Flegrei caldera, Southern Italy". *Geological Society of America*, Special Paper, pp. 263.
- Dvorak, J.J. and Berrino, G. (1991) "Recent ground movement and seismic activity in Campi Flegrei, Southern Italy: episodic growth of a resurgent dome", *Journal of Geophysical Research*, **96**, 2309-2323.
- Gaeta, F.S., De Natale, G., Peluso, F., Mastrolorenzo, G., Castagnolo, D., Troise C., Pingue, F., Mita, D.G. and Rossano, S. (1998), "Genesis and evolution of unrest episodes at Campi Flegrei caldera: the role of thermal-fluid-dynamical processes in the geothermal system", *Journal of Geophysical Research*, **103** (B9), 20921-20933.
- Itasca Consulting Group Inc. (1997), "FLAC3D Manual: Fast Lagrangian Analysis of Continua in 3 dimensions – Version 2.0", *Itasca Consulting Group Inc.*, Minnesota, USA.
- Martini, M. (1986), "Thermal activity and ground deformation at Phlegrean Fields, Italy: precursors of eruptions or fluctuations of quiescent volcanism? A contribution of geochemical studies", *Journal of Geophysical Research*, **91**, 12,255-12,260.
- Martini, M., Giannini, L., Buccianti, A., Prati, F., Cellini Legittimo, P., Bozzelli, P. and Capaccioni, B. (1991), "1980-1990: ten years of geochemical investigation at Phlegrean Fields (Italy)", *Journal of Volcanology and Geothermal Research*, **48**, 161-171.
- Olivieri del Castillo, A. and Quagliariello, M.T. (1969), "Sulla genesi del bradisismo flegreo", *Atti Associazione Geofisica Italiana*, 18<sup>mo</sup> Congresso, Napoli, pp.557-594.
- Orsi G., Petrazzuoli, S.M. and Wohletz, K. (1999), "Mechanical and thermo-fluid behaviour during unrest at the Campi Flegrei caldera (Italy)", *Journal of Volcanology and Geothermal Research*, **91**, 453-470.
- Panichi, C. and Volpi, G. (1999), "Hydrogen, oxygen and carbon isotope ratios of Solfatara fumaroles (Phlegrean Fields, Italy): further insight into source processes", *Journal of Volcanology and Geothermal Research*, **91**, 321-328.
- Parascandola, A. (1947), "I fenomeni bradisismici del Serapeo di Pozzuoli", Genovese, Napoli.
- Pruess, K. (1991), "TOUGH2 – A general purpose numerical simulator for multiphase fluid and heat flow", Lawrence Berkeley Nat. Lab. *Report LBL 29400*.
- Rutqvist, J., Wu Y.-S., Tsang, C.-F. and Bodvarsson, G. (2002), "A modelling approach for analysis of coupled multiphase fluid flow, heat transfer, and deformation in fractured porous rock", *International Journal of Rock Mechanics*, **39**, 429-442.
- Tedesco, D. and Scarsi, P. (1999), "Chemical (He, H<sub>2</sub>, CH<sub>4</sub>, Ne, Ar, N<sub>2</sub>) and isotopic (He, Ne, Ar, C) variations at the Solfatara crater (Southern Italy): mixing of different sources in relation to seismic activity", *Earth and Planetary Science Letters*, **171**, 465-480.
- Tedesco, D., Allard, P., Sano, Y., Wakita, H. and Pece, R. (1990), "Helium-3 in subaerial and submarine fumaroles of Campi Flegrei caldera, Italy", *Geochimica et Cosmochimica Acta*, **54**, 1105-1116.
- Todesco, M., Chiodini, G. and Macedonio, G. (in press), "Monitoring and modeling hydrothermal fluid emission at La Solfatara (Phlegrean Fields, Italy). An interdisciplinary approach to the study of diffuse degassing", *Journal of Volcanology and Geothermal Research*.